CLM-R 21

United Kingdom Atomic Energy Authority

RESEARCH GROUP

Report

THE ROLE OF HALL CURRENTS AND PLASMA VORTICES IN THE PLANAR CURRENT SHEET IN A COAXIAL PLASMA ACCELERATOR

W. H. BOSTICK

Culham Laboratory,

Culham, Abingdon, Berkshire

1962

U.D.C.
533.951

The Role of Hall Currents and Plasma Vortices in the Planar Current Sheet in a Coaxial Plasma Accelerator

By

W. H. BOSTICK*
Stevens Institute of Technology, Hoboken, N.J.

ABSTRACT

The fact that the current sheet in a coaxial plasma accelerator[1,2,3] is planar when the center conductor is negative and bullet-shaped when the center conductor is positive can be explained at least partially by a combination of Hall currents and plasma vortices[4], both of which should be expected to occur in such an accelerator. This explanation asserts that the peculiar asymmetrical behaviour of this accelerator is a consequence of the fundamental property of ordinary-matter plasma; that electrons are light and positive ions are heavy. The sign of the asymmetry would be changed if anti-matter plasma were employed. It is doubtful whether a planar current sheet could be achieved with a positronium plasma.

* On a NSF Fellowship at Euratom - CEA, Fontenay-aux-Roses, France and the Culham Laboratory, Culham, England.

U.K.A.E.A. Research Group,
Culham Laboratory,
Nr. Abingdon,
Berks.
August, 1962

1. The excellent experimental work and analysis by Burkhardt and Lovberg[1] have rendered a good beginning for the understanding of the operation of the coaxial plasma accelerator. This present paper describes the roles which the Hall effect and plasma vortices[4] will be expected to play. These roles make the understanding of the experimental facts more complete. The Hall effects and plasma vortices also help explain the results of Keck et al[2,3] who find (as do Burkhardt and Lovberg) that the current sheet is planar when the center conductor is the cathode but who find, in addition, that the current sheet is non-planar (bullet-shaped) when the center conductor is the anode.

2. Some of the measurements by Burkhardt and Lovberg[1] of B_θ, Ex, and Er in the plasma are displayed schematically in Fig. 1(c,d and e). Because the plasma in the current sheet and in the region following the current sheet (where radial currents also are flowing) is under acceleration by $\mathbb{J}_r \times B_\theta$ forces, where $\mathbb{J}_r$ is carried primarily by electrons, the lagging positive ions set up the axial electric field E_x. The curious dip in the measured E_x, in the region B not explained by Burkhardt and Lovberg, may be explained by a mass circulation pattern, v_e, shown in Fig.1(b). The electric field E_x may be expected to drive Hall currents in the regions A and C in Fig.1(a) as shown. The braking of the velocity shear immediately behind the current sheet is expected to produce the Hall current pattern shown in the region B, Fig.1(a).

3. A quantitative model which describes the build up of this mass circulation pattern (vortices) and the Hall currents will now be set forth. This model assumes a current sheet of thickness δ which is to act like a shock. The author recognises that the radial current flows behind this current sheet as well as in it, and that the quantities of B_θ, E_x, E_r and mass velocity actually vary continuously in and behind the shock, but for simplicity in exposition it is necessary, at this stage of the art, to assume a current sheet of thickness δ as a shock. The following flow equations, for any value of r, $a < r < b$, can be written down in the frame of reference of the current sheet at that particular r. The "unshocked" plasma enters the shock from the right with a velocity $\dot{x}_1$, and density n_1, as shown in Figs.1(b) and 2, and leaves with values of velocity and density which are denoted by a subscript 2.

Mass flow:
$$n_1 m_i \vec{\dot{x}}_1 = n_2 m_i \vec{\dot{x}}_2 + n_2 m_i \vec{\dot{r}}_2 \tag{1}$$

Momentum flow:
$$n_1 m_i \dot{x}_1^2 - \frac{B_2^2}{2\mu_o} = n_2 m_i \dot{x}_2^2 + (n_2 kT_2 - n_1 kT_1) \tag{2}$$

$$- \delta \frac{W_\perp}{B} \frac{dB}{dr} - \delta \frac{d}{dr}(nkT) = n_2 m_i \dot{r}_2 \dot{x}_2 \tag{3}$$

Energy flow:
$$\dot{x}_1 \left[\frac{n_1 m_i \dot{x}_1^2}{2} + n_1 kT_1\right] + \dot{x}_1 n_1 kT_1 - \dot{x}_2 n_2 kT_2 - \frac{B_2^2}{2\mu_o} = \dot{x}_2 \left[\frac{n_2 m_i \dot{x}_2^2}{2} + n_2 kT_2 + \frac{n_2 m_i \dot{r}_2^2}{2} + \frac{B_{\theta p}^2}{2\mu_o}\right]. \tag{4}$$

4. The measurements of Bur hardt and Lovberg indicate that at $r \cong a$ (i.e. near the surface of the inner conductor $e\int_o^\delta E_x dx \cong eE_x\delta \cong \frac{m_i x_1}{2}$ and that here x_2 is small. Thus, for $r \cong a$ in equation (2), the $n_2 m_i \dot{x}_2^2$ term can be neglected, and

$$n_1 m_i \dot{x}_1^2 = \frac{B_2}{2\mu_o} = n_1 \dot{x}_1 e\int E_x dt \cong \frac{x_1 n_1 \delta E_x}{\frac{\dot{x}_1}{2}} = 2n_1 eE_x\delta \qquad (5)$$

Thus

$$eE_x = \frac{B_2^2}{2\mu_o} \cdot \frac{1}{2n_1\delta}. \qquad (6)$$

The pressure $n_2kT_2 - n_1kT_1$ is neglected in equation (2).

5. The field E_x is expected to be set up by the acceleration of the positive ions, such that $E_x = m_i\ddot{x} = m_i\ddot{x}_1$. This can be seen quited clearly by differentiating equation (5) by x_1. Thus

$$\frac{d}{dx_1}(n_1 m_i \dot{x}_1^2) = \frac{dt}{dx_1}\frac{d}{dt}(n_1 m_i \dot{x}_1^2) = \frac{2n_1 m_i \dot{x}_1 \ddot{x}_1}{\dot{x}_1} = \frac{d}{dx}\frac{B_a^2}{2\mu_o}$$

$$\cong \frac{B_2^2}{2\mu_o\delta} \quad \text{or} \quad m_i\ddot{x}_1 = \frac{B_2^2}{2\mu_o} \cdot \frac{1}{2n_1\delta}.$$

Then by equation (6) $\qquad eE_x = m_i\ddot{x}_1 = m_i\ddot{x}$

6. If the value of $B_2 (= B_\theta)$ at $r = a$ at the left-hand border of the current sheet is $B_2 = B_o \sin\omega t$, the value at $r = r$ is $B_2 = \frac{a}{r} B_o \sin\omega t$, in the absence of any axial electrical currents in the plasma.

Thus $\qquad E_x(r,t) = \frac{a^2}{r^2} \frac{B_o^2 \sin^2\omega t}{2\mu_o \, 2n_1\delta}$ and if $\dot{x}_2 \cong o$ at $r = a$, $\dot{x}_3 > o$

for $r > a$ for a planar current sheet. Indeed equation (2) tells us that for $r = b$

$$n_1 m_i \dot{x}_1^2 - \frac{a^2}{b^2}\frac{B_o^2 \sin^2\omega t}{2\mu_o} = n_2 m_i \dot{x}_2^2 \qquad (7)$$

This equation combined with equation (2) for $r = a$ gives

$$n_2 m_i \dot{x}_2^2(b) = \frac{B_o^2 \sin^2\omega t}{2\mu_o}\left(1 - \frac{a^2}{b^2}\right), \qquad (8)$$

and

$$\frac{n_2 m_i \dot{x}_2^2(b)}{n_1 m_i \dot{x}_1^2} = 1 - \frac{a^2}{b^2} \qquad (9)$$

7. Now equation (1) shows obviously that at $r = a$ there will have to be some radial velocity unless n_2 is permitted to become infinite, which is unlikely. Figs.1(b) and 2(a) attempt to show both the velocities $\dot{x}_2$, $\dot{r}_2$ and their resultants at various values of $a < r < b$ in the frame of reference of the planar current sheet whose velocity $\dot{x} = -\dot{x}_1$ and whose $\dot{x}_2 = o$ at $r = a$. At $r = b$ there can be no $\dot{r}_2$ and all of the mass flow in the shocked plasma must be in the $\dot{x}_2$

direction. Thus at r = b from equation (1)

$$n_1 m_i \dot{x}_1 = n_2 m_i \dot{x}_2(b) \tag{10}$$

Equation (10) combined with equation (9) gives

$$\frac{\dot{x}_2(b)}{\dot{x}_1} = 1 - \frac{a^2}{b^2} = \frac{n_1}{n_2(b)} \tag{11}$$

at r = b. At values of r < b equation (1) demands values of $n_2(r) > n_2(b)$ unless a flow velocity $\dot{r}_2$ is permitted. The buildup of n at r < b within the current sheet gives rise to a pressure term $-\delta$ grad nkT $= -\frac{\delta d}{dr}(nkT)$. This pressure term and the radial gradient in magnetic field $\frac{dB}{dr}$, tend to produce the flow in the $\dot{r}_2$ direction as indicated in equation (3). $W_\perp$ is the plasma thermal energy perpendicular to the magnetic field. It is to be expected that the flow in the $\dot{r}_2$ direction, especially for values of r near a will relieve the very high values of n_2 which would otherwise occur there, and that eventually in the region some distance behind the current sheet the radial variation in n_2 will adjust itself so that $n_2 kT_2 + \frac{a^2}{r^2} \frac{B_o^2 \sin^2 \omega t}{2\mu_o}$ = constant.

8. The shear in velocity $\dot{x}_2$ as a function of r is shown diagrammatically in Fig.1(b) and also in Fig.2 where the diagram is enlarged and where the values of $\dot{x}_2$ are shown for the reference frame of the current sheet which moves at a velocity $-\dot{x}_1$ (Fig.2(a), and for a reference frame which moves with a velocity in the x direction corresponding to the shocked material at $r \simeq \frac{a+b}{2}$ (Fig.2(b)). In the shocked plasma to the left of the current sheet, the shear in the velocity in conjunction with the B_θ (in the direction shown in Figs. 1 and 2) will produce Hall currents in this plasma in the + and - x directions as shown in region B, Fig.1(a). These Hall currents crossed with B_θ produce the necessary forces in the + and - r directions to close the flow of plasma into an eddy or several eddies as suggested in Fig.1(b). A very significant point is the fact that only when the center conductor of the coaxial accelerator is <u>negative</u> can B_θ be in the <u>correct direction</u> to close this shear in the velocities into an eddy in region B. If B_θ is of the opposite sign, as it will be when the center conductor is positive, then the shear in the velocities $\dot{x}_2$ will throw the plasma toward the electrodes. The setting up of this eddy pattern when the center conductor is negative is suggested as a crucial ingredient in the production and maintenance of the planar current sheet reported by Burkhardt and Lovberg and Keck et al. when the center conductor is negative.

9. The transient growth of the shear in the velocities $\dot{x}_2$ can be obtained from

$$\dot{x}_2(b) - \dot{x}_2(a) \cong \dot{x}_2(b) = \left[\frac{B_o^2 \sin^2 \omega t}{n_2 m_i \cdot 2\mu_o} \left(1 - \frac{a^2}{b^2}\right) \right]^{\frac{1}{2}} = \frac{B_o \sin \omega t \left(1 - \frac{a^2}{b^2}\right)}{(n_1 m_i \cdot 2\mu_o)^{\frac{1}{2}}}$$

10. We now examine the energy flow as set forth in equation (4). For simplicity it will be assumed that both $n_1 kT_1$ and $n_2 kT_2$ can be neglected. If $\dot{x}_2$ actually approaches zero as $r \to a$ it would be necessary for n_2 to approach infinity to satisfy equation (4). Obviously $\dot{x}_2$ must be finite, though small at $r = a$ and hence the "snow plow" which is certainly permeable for values of $r > a$ also must leak somewhat for $r = a$.

11. Furthermore, in order to balance the energy on the left side of equation (4), there must be finite energy terms such as $\frac{\dot{x}_2 n_2 m_i r_2^2}{2}$ and $\frac{\dot{x}_2 B_{\theta p}^2}{2\mu_o}$ on the right side of the equation. For example for a ratio of $\frac{a}{b} = \frac{1}{2}$, $\frac{n_2(b)}{n_1} = \left(1 - \frac{a^2}{b^2}\right)^{-1} = \frac{4}{3}$.

12. We assme that $n_2(r) \cong n_2(b)$ for $a < r < b$. To obtain $\dot{x}_2(r)$ we combine equation (10) written for $\dot{x}_2(r)$ instead of $\dot{x}_2(b)$ and equation (9) also written for $\dot{x}_2(r)$. Thus $\dot{x}_2(r) = \left(1 - \frac{a^2}{r^2}\right)\dot{x}_1$. Also since $\frac{B_2^2}{2\mu_o} = \frac{B_o^2 \sin^2\omega t}{2\mu_o} \cdot \frac{a^2}{r^2}$ and $n_1 m_i \dot{x}_1^2 - \frac{B_o^2 \sin^2\omega t}{2\mu_o} \cong 0$ from equation (2), the energy equation (4) can be written

$$n_1 m_i \dot{x}^3 \left[\frac{1}{2} - \frac{a^2}{r^2}\left(1 - \frac{a^2}{r^2}\right)\right] = \frac{4}{3} n_1 m_i \dot{x}^3 \left(1 - \frac{a^2}{r^2}\right)^3 + \dot{x}_1 \left(1 - \frac{a^2}{r^2}\right)\left[\frac{n_2 m_i r_2^2}{2} + \frac{B_{\theta p}^2}{2\mu_o}\right] \qquad (12)$$

For example for the value $\frac{a}{r} = \frac{1}{1.5}$ equation (12) becomes

$$n_1 m_i \dot{x}_1^3 (0.254) = \underbrace{n_1 m_i \dot{x}_1^3 (0.227)}_{\text{translation energy}} + \underbrace{\dot{x}\left(1 - \frac{a^2}{r^2}\right)\left[\frac{n_2 m_i \dot{r}_2^2}{2} + \frac{B_{\theta p}^2}{2\mu_o}\right]}_{\text{rotational and magnetic energy}} \qquad (13)$$

Thus <u>in the frame of reference of the current sheet</u>, at the value of $r = 1.5a$ for a coaxial gun whose $\frac{a}{b} = \frac{1}{2}$, the fraction of the incoming kinetic energy which remains as kinetic energy of translation, i.e. as $\frac{n_2 m_i \dot{x}_2^3}{2}$, is $\frac{0.227}{0.254}$ or 90%. The fraction which is converted to rotational kinetic energy and magnetic field is 10%.

13. The velocity $\dot{x}(1.5a)$ in the laboratory frame of reference is

$$\dot{x}(1.5a) = \dot{x}_1 - \dot{x}_2(1.5a) = \dot{x}_1\left[1 - \left(1 - \frac{1}{(1.5)^2}\right)\right] = 0.445\dot{x}$$

Then

$$\frac{\frac{1}{2} n_2 m_i \dot{x}^2}{\frac{1}{2} n_2 m_i \dot{x}_2^2} = \left(\frac{0.445}{0.555}\right)^2 = 0.64$$

is the ratio in the laboratory frame and the current sheet frame of the kinetic energy of translation of the material immediately behind the shock at $r = 1.5a$ and where $\frac{a}{b} = \frac{1}{2}$. Thus the ratio of rotational and magnetic energy

in equation (13) to kinetic energy of translation in the laboratory system is 17% by this form of estimate.

14. A very rough estimate of the ratio of the rotational kinetic energy in the eddy to the translational kinetic energy of the eddy in the laboratory system can be made in another way as follows: the kinetic energy of translation of the eddy, of volume V, in the region immediately behind the current sheet is

$$\tfrac{1}{2}n_2 m_i \dot{x}^2 V \simeq \tfrac{1}{2}n_2 m_i V(\dot{x}_1 - \dot{x}_2(1.5a))^2 = \tfrac{1}{2}n_2 m_i V\dot{x}_1^2 \left[1 - \left(1 - \frac{1}{(1.5)^2}\right)\right]^2$$

$$= \tfrac{1}{2}n_2 m_i V\dot{x}_1^2 \ (0.445)^2$$

15. The value of $\dot{x}_2$ has been taken as that for $r = 1.5a$ and, as before, $\frac{a}{b} = \frac{1}{2}$. The kinetic energy of rotation can be estimated roughly as that for $\frac{1}{3}$ of the same mass rotating with the full peripheral rotational velocity. Thus the kinetic energy of rotation is roughly $\frac{1}{3} \cdot \frac{1}{2}n_2 m_i V\left[\frac{x_2(b)}{2}\right]^2 = \frac{1}{3} \cdot \frac{1}{2}\, n_2 m_i \dot{x}^2 V\left[\cdot\frac{75}{2}\right]^2$. The ratio of kinetic energy of rotation to kinetic energy of translation in the laboratory system of the eddy immediately behind the shock is, according to this rough estimate, $\frac{1}{3}\left(\frac{0.375}{0.445}\right)^2 = 23\%$. The plasma in this eddy will be eventually accelerated up to the full average translational speed of $\frac{E_r \times B_\theta}{B_\theta^2}$ by the time it has passed into the region D in Fig.1(a).

16. Thus the "increase of entropy" in this shock instead of going primarily into $n_2 kT_2$ goes (at least in part) into the production of kinetic energy of rotation in the eddy and into a perturbation B_θ, $B_{\theta p}$.

17. Now the axial electric field, E_x, can produce the Hall current circulation pattern within the current sheet itself shown in Fig.1(a) with the resultant build up of $B_{\theta p}$, the perturbation B_θ. The rate of build up of these particular Hall currents in the region A can be roughly computed in the following way. The effective EMF in the circulation pattern of Hall currents is approximately $E_x\delta$ where E_x will be taken as the value for $r \simeq a$. Inductances L_1 and L_2 for the two current loops can be assigned, with the assumption that the Hall currents producing $B_{\theta p}$ flow primarily on the periphery of the loops shown in Fig.2(b). It is probable that the return circuit for the Hall currents is mainly through the metal electrode walls as shown in Fig. 2(b). The lumped inductances L_1 and L_2 may be expected to be roughly

$$L_1 \cong \tfrac{1}{3}\left(\frac{b-a}{4}\right)\frac{\delta\mu_o}{2\pi a},$$

and

$$L_2 \cong \tfrac{1}{3} \cdot \frac{\frac{3}{4}(b-a)\delta\mu_o}{\frac{2\pi(a+b)}{2}} \cong \tfrac{1}{2}\frac{(b-a)\delta\mu_o}{2\pi(a+b)} \qquad (15)$$

Since E_x in the region of r = a is approximately $\frac{B_o^2 \sin^2 \omega t}{e 2\mu_o \cdot 2n_1 \delta}$, the emf which drives current in these loops is

$$E_x \delta \cong \frac{B_o^2 \sin^2 \omega t}{4e\mu_o n_1} \tag{16}$$

The effective resistance of the metal and plasma-to-metal contact will be given by R_{m_1} and the effective plasma resistance by R_{p_1} for loop number 1. The equation then for the build up of the current i_1 in loop number 1, for example, is

$$\frac{B_o^2 \sin^2 \omega t}{4e\mu_o n_1} = \frac{L_1 di_1}{dt} + (R_{m_1} + R_{p_1}) i_1 \tag{17}$$

During the early portion of the period when $\sin \omega t \cong \omega t$ and the current is limited primarily by L_1 and not by $(R_{m_1} + R_{p_1})$

$$\frac{di_1}{dt} \cong \frac{B_o^2 \omega^2 t^2}{4L_1 e\mu_o n_1} \tag{18}$$

and

$$i_1 \cong \frac{B_o^2 \omega^2 t^3}{12L_1 e\mu_o n_1} \qquad i_2 = \frac{B_o^2 \omega^2 t^3}{12L_2 e\mu_o n_1}$$

It can be seen that i_1 and i_2 and hence $B_{\theta p}$ grow rapidly with t in the beginning. This energy stored in $B_{\theta p}$ is passed on to the shocked plasma and hence forms a portion of the energy transported away from the current sheet, as indicated in equation (4).

18. It is noteworthy that when the center conductor of the coax is <u>negative</u>, the perturbation magnetic fields, $B_{\theta p}$, produced by i_1 and i_2, are in such a direction as to partially compensate the variation of $B_2 = \frac{aB_o \sin \omega t}{r}$ with $\frac{1}{r}$. If the center conductor is positive the values of $B_{\theta p}$ accentuate the variation of B_2 with $\frac{1}{r}$. However, the $\mathbb{J}_H \times B_\theta$ forces along the rear border of the current sheet in region A in Figs.1(b) and 2(b) are such as to accentuate the development of the shear in the $\dot{x}_2$ when the center conductor is negative; and the algebraic sum of the $\mathbb{J}_H$ in the region A, Figs.1(a) and 2(b), and the radial currents driven by the applied voltage produces a current pattern which tends to be the opposite of the bullet shape.

19. This asymmetry in the behaviour of the coaxial accelerator has an interesting parallelism with non-conservation of parity in weak interactions[7]. The character of the asymmetry should change sign if anti-matter plasma is substituted for the ordinary-matter plasma, because the sign of the asymmetry with ordinary matter depends upon the fact that positive ions are heavy and electrons are light. The same type of asymmetry in the production of plasmas which show lefthandedness has been observed[8].

20. Further analytical and experimental work on the processes which transpire in the current sheet itself is necessary before this current sheet can be really understood. Indeed the measurements of Keck et al[2,3] indicate that the current sheet is broad, covering about 5 cm in argon.

ACKNOWLEDGMENTS

21. The author wishes to express his especial gratitude and indebtedness to John Nankivell, whose frequent correspondence on his experimental work (for a doctoral thesis at Stevens) on the coaxial plasma accelerator has provided the motivation and inspiration for this paper. The author also wishes to thank the National Science foundation providing the fellowship under which this work was performed, and the EURATOM-CEA at Fontenay-aux-Roses and the Culham Laboratory where the author has been stationed during the fellowship.

REFERENCES

(1) Burkhardt, L.C. and Lovberg, R.H.
Current sheet in a coaxial plasma gun.
Physics of Fluids, vol.5, no.3, pp.341-347, March, 1962.

(2) Keck, J.C.
Current distribution in a magnetic annular shock tube.
Physics of Fluids, vol.5, no.5, pp.630-632, May, 1962.

(3) Fishman, F.J. and Petschek, H.
Flow model for large-radius ratio magnetic annular shock-tube operation.
Physics of Fluids, vol.5, no.5, pp.632-633, May, 1962.

(4) Bostick, W.H.
Measurement of the properties of plasma eddies produced by shear in velocity in a magnetic field.
Euratom-CEA report no.EUR-CEA-FC-150, August, 1962.

(5) Bostick, W.H.
Experimental study of ionized matter projected across a magnetic field.
Physical Review, 2nd series, vol.104, no.2, pp.292-299, October 15, 1962.

(6) Bostick, W.H.
Experimental study of plasmoids.
Physical Review, 2nd series, vol.106, no.3, pp.404-412, May 1, 1957.

(7) Lee, T.D. and Yang, C.N.
Question of parity conservation in weak interactions.
Physical Review, 2nd series, vol.104, no.1, pp.254-258, October 1, 1956.

(8) Bostick, W.H.
On the non-conservation of parity in the production of plasmoids.
Euratom-CEA report no. EUR-CEA-FC-176, August, 1962.

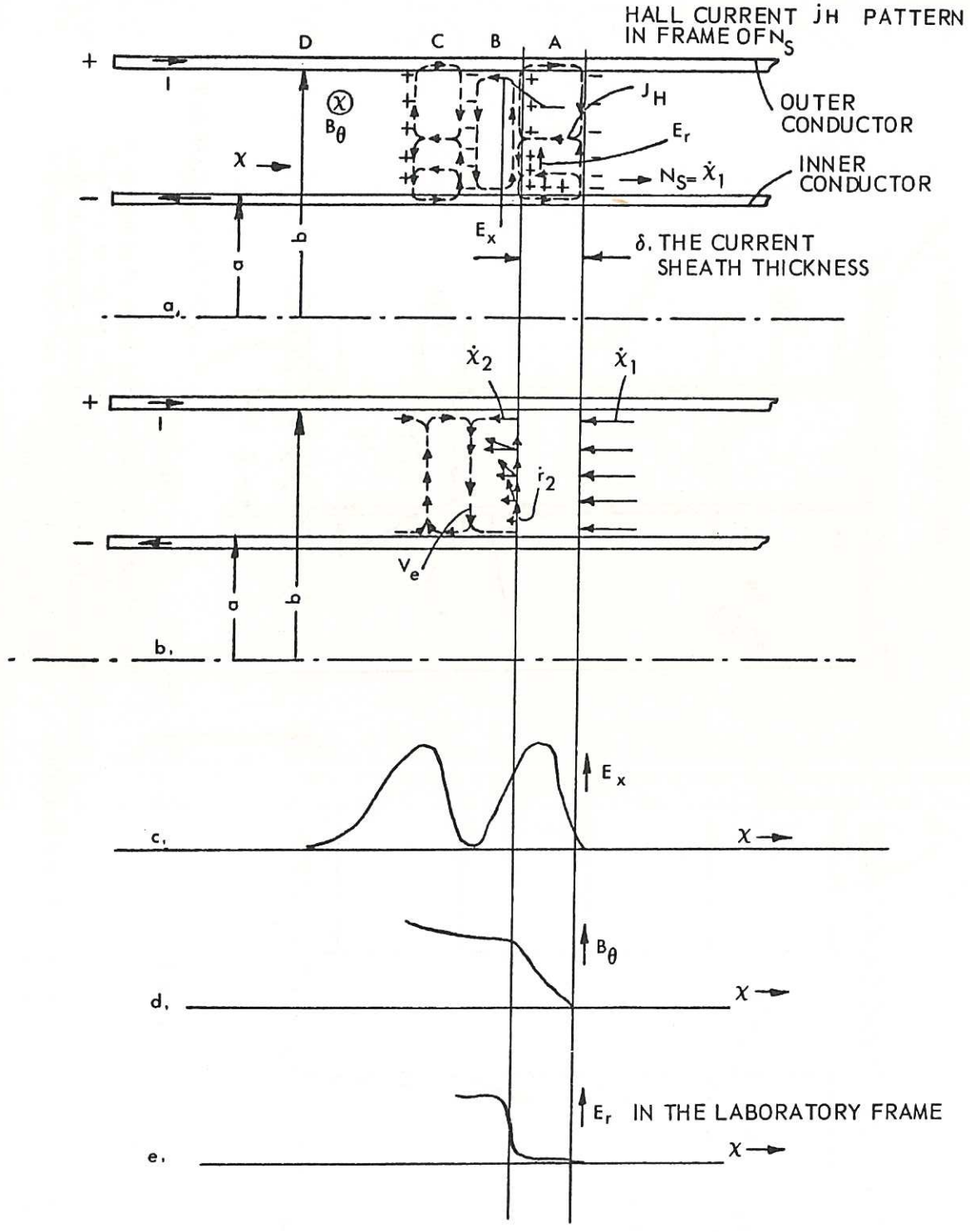

CLM - R 21 Fig. 1 Suggested Hall current J_H and mass eddy pattern v_e to help explain the experimental profiles E_x, B_θ and E_r.

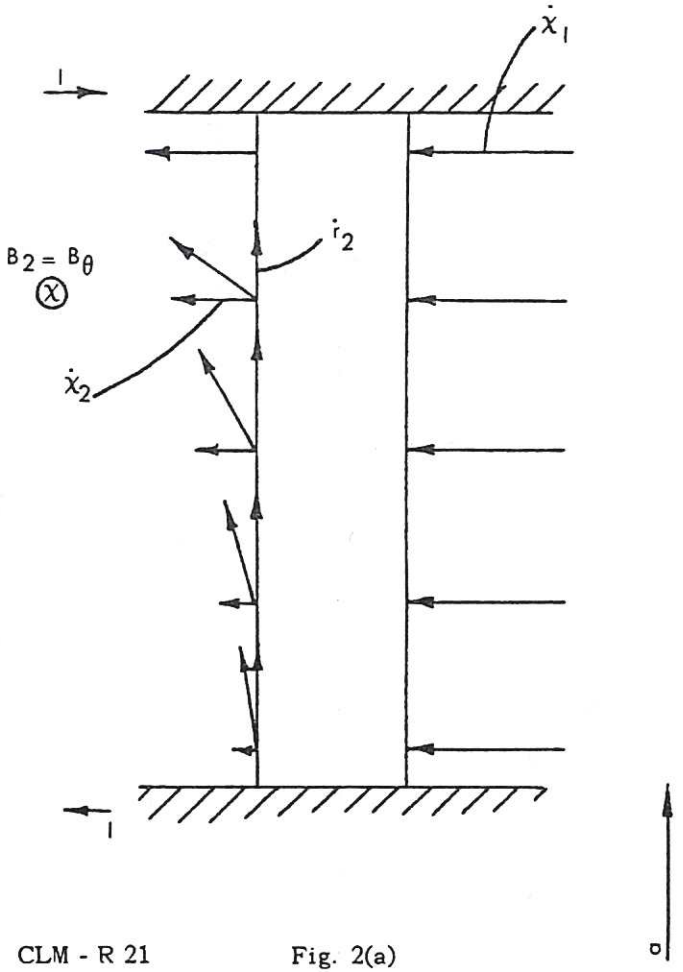

CLM - R 21 Fig. 2(a)

Enlarged view of the velocities $\dot{x}_2$, $\dot{r}_2$ and $\dot{x}_1$ in the frame of reference of the current sheet.

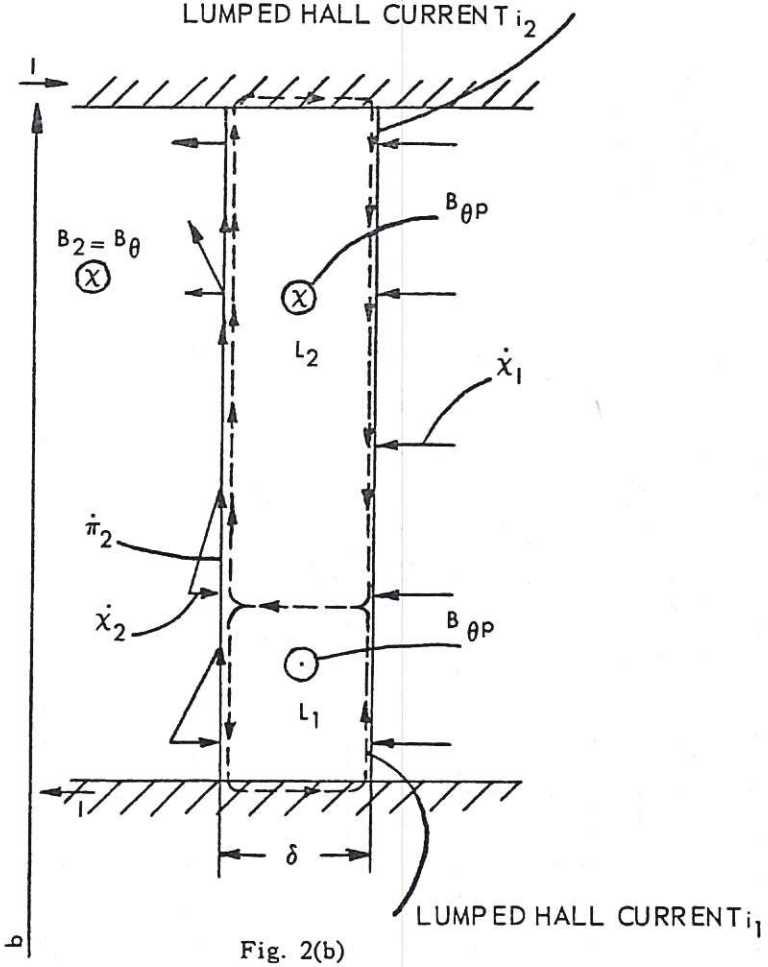

Fig. 2(b)

The velocities $\dot{x}_2$ and $\dot{r}_2$ in the frame of reference of the translational velocity of the plasma at $r = \frac{a+b}{2}$ The circulation of the lumped Hall currents in the current sheet along with their perturbation magnetic fields $B_{\theta p}$ is also shown.